GCR flux 9-day variations with LISA Pathfinder

IOP Conf. Series: Journal of Physics: Conf. Series **840** (2017) 012037 doi:10.1088/1742-6596/840/1/012037

GCR flux 9-day variations with LISA Pathfinder

C Grimani[1,2] for the LISA Pathfinder Collaboration

and S Benella[1,2], M Fabi[1], N Finetti[2,3], D Telloni[2,4]

[1] DiSPeA, University of Urbino, 61029 Urbino, Italy
[2] National Institute for Nuclear Physics (INFN), Section in Florence, 50019 Sesto Fiorentino, Italy
[3] Department of Physical and Chemical Sciences, University of L'Aquila, 67100 L'Aquila, Italy
[4] National Institute for Astrophysics, Astrophysical Observatory of Torino, 10025 Pino Torinese, Italy

E-mail: `catia.grimani@uniurb.it`

Abstract. Galactic cosmic-ray (GCR) energy spectra in the heliosphere vary on the basis of the level of solar activity, the status of solar polarity and interplanetary transient magnetic structures of solar origin. A high counting rate particle detector (PD) aboard LISA Pathfinder (LPF) allows for the measurement of galactic cosmic-ray and solar energetic particle (SEP) integral fluxes at energies > 70 MeV n^{-1} up to 6500 counts s^{-1}. Data are gathered with a sampling time of 15 s. A study of GCR flux depressions associated with the third harmonic of the Sun rotation period (~ 9 days) is presented here.

1. Introduction

Solar activity level and Global Solar Magnetic Field (GSMF) polarity modulate galactic cosmic-ray (GCR) fluxes in the heliosphere (see for instance [1, 2, 3, 4, 5]). A direct correlation between high solar activity and solar energetic particle (SEP) event occurrence is also observed [6, 7].

The symmetric model in the *force field approximation* by Gleeson and Axford [8] allows for the estimate of the energy spectra of cosmic rays at a distance r from the Sun, at a time t during periods of positive polarity, when time-independent interstellar intensities are assumed. An energy loss related to the charge of cosmic-ray particles and a *solar modulation parameter*, ϕ, above about 100 MeV are considered. The role played by the GSMF polarity on the drift of positive (negative) particles in the heliosphere during periods of negative (positive) polarity must be also taken properly into account. Protons and nuclei reaching Earth during negative polarity periods come mainly from the ecliptic regions along the Heliospheric Current Sheet (HCS). An opposite situation holds during positive magnetic field polarity periods when positive particles come from the polar region of the Sun. Particles propagating along the HCS lose more energy than those coming from the poles.

Nominal quasiperiodicities of 27, 13.5 and 9 days related to the Sun rotation period and its higher harmonics are also observed in the cosmic-ray flux, the interplanetary magnetic field (IMF), the solar wind plasma and the geomagnetic activity parameters [9]. GCR observations gathered in space above a few tens of MeV by Helios 1, Helios 2 and IMP-8 experiments indicated that the effects of corotating interaction regions, generated by high-speed solar wind streams

overtaking preceding slower solar wind, are at the origin of the 9-day GCR modulations [10]. A high counting rate particle detector (PD) aboard LISA Pathfinder (LPF) presents a typical response of more than 100 counts s^{-1} in 15 s sampling time, allowing for limiting the statistical uncertainty on one-hour binned GCR proton and helium nucleus flux data at percent level above 70 MeV n^{-1}. The aim of this work is to report on the characteristics of $\sim$ 9-day GCR short-term variations, compatible with the third harmonic of the solar rotation period, during the first three months of the LPF mission.

2. The Particle Detector aboard LPF

LPF [11, 12, 13] is the ESA (European Space Agency) key technology demonstrator mission for LISA [14], the first interferometer devoted to gravitational wave detection in space. The LPF spacecraft was successfully launched from the Kourou base in French Guiana on December 3rd, 2015 aboard a Vega rocket. The satellite reached its six-months, final orbit around the Earth-Sun Lagrangian point L1 at about 1.5 million km from Earth on January 2016. The LPF orbit is inclined at about 45 degrees on the ecliptic plane. Orbit minor and major axes are approximately of 0.5 million km and 0.8 million km, respectively. LPF carries two 2-kg cubic platinum-gold free-floating test masses that play the role of mirrors of the interferometer. The charging process due to GCRs and SEPs results in spurious force noise on both test masses [15]. The effects of the charging process were properly estimated before the mission launch with Monte Carlo simulations [16, 17] carried out on the basis of GCR and SEP occurrence projections for the period orbits about the L1 point [18]. The minimum energy of protons and ions (98% in composition of both GCRs and SEPs [19]) penetrating and charging the LPF test masses is 100 MeV n^{-1}. The conservative choice of monitoring GCR above 70 MeV n^{-1} on LPF was made in order not to underestimate the overall particle flux charging the test-masses. The LPF PD is mounted behind the spacecraft solar panels and oriented along the Sun-Earth direction. This device consists of two, 300 μm thick, silicon wafers of 1.4 x 1.05 cm^2 area, separated by 2 cm and placed in a telescopic arrangement [20, 21]. For particle energies $>$ 100 MeV n^{-1} the instrument geometrical factor is found to be energy independent and equal to 9 cm^2 sr for particle isotropic incidence on each silicon wafer. In coincidence mode the detector geometrical factor is about one tenth of this value. A shielding, copper box surrounds the silicon wafers. The box thickness is 6.4 mm. This shielding material stops particles with energies smaller than 70 MeV n^{-1}. The PD allows for the counting of particles crossing each silicon layer and for the measurement of ionization energy losses of particles passing through both silicon wafers (coincidence mode). The PD data are stored in the form of histograms over periods of 600 s and then sent to the on-board computer. The maximum allowed PD counting rate is 6500 counts s^{-1}, corresponding to an event integrated proton fluence of 10^8 protons cm^{-2} at energies $>$ 100 MeV. In coincidence mode, up to 5000 energy deposits per second can be stored in each histogram. The expected occurrence of SEP events with fluence $> 10^8$ protons cm^{-2} at energies $>$ 30 MeV, for instance, is less than 1 per year as it follows from the Nymmik model [22]. None of SEP events, characterized by proton differential fluxes above 100 MeV n^{-1} overcoming that of galactic origin, were observed since the LPF launch and up to the time of writing. This scenario makes the whole period of the LPF mission the most favourable for GCR short-term variation investigation. Data from the PD are available since mid-February 2016.

3. GCR and interplanetary solar wind plasma parameter short-term variations

The parameterization of the GCR energy spectra adopted here follows from the work by Papini, Grimani & Stephens [19]:

$$F(E) = A\ (E+b)^{-\alpha}\ E^{\beta} \quad \text{particles}/(\text{m}^2\ \text{sr}\ \text{s}\ \text{GeV/n}). \tag{1}$$

The values of the parameters A, b, α and β for proton and helium nucleus energy spectra at the beginning of the LPF mission (corresponding to a solar modulation parameter ϕ=550 MV c^{-1} [23]) appear in Table 1.

Table 1. Parameterization of proton and helium energy spectra during the first part of the LPF mission.

	A	b	α	β
p	18000	1.19	3.66	0.87
He	850	0.96	3.23	0.48

The fractional variations of GCR fluxes of duration compatible with a 9-day periodicity corresponding to the third harmonic of the Sun rotation period, observed with the LPF PD during the Bartels rotations 2490-2492 (February 6th, 2016 - April 27th, 2016) are shown in Figs. 1 - 6. In Figs. 1, 3 and 5 GCR data are compared to the magnetic field and solar wind plasma parameters gathered simultaneously in L1 by the ACE experiment [24]. A striking majority of the observed GCR flux depressions show longer recovery than decrease periods and appear correlated with the interplanetary magnetic field intensity above 10 nT (fourth and bottom panels in Figs. 1-3-5) and solar wind plasma speed above 400 km s^{-1} (second and bottom panels in figures 1-3-5). HCS crossing is also indicated in the middle panels of figures 1-3-5. HCS are modulated by incoming high-speed solar wind streams. Changes of IMF polarity associated with plasma density enhancements are observed when LPF crosses the HCS. In Figs. 2-4-6 the LPF GCR flux fractional variations are compared to analogous polar and near-polar neutron monitor observations. The stations considered here present vertical geomagnetic cutoffs < 0.8 GV c^{-1} and effective energies > 5.5 GeV. It is worthwhile to recall that neutron monitors allow for a direct measurement of the GCR flux at energies larger than the effective energy, when fractional variations of neutron monitor countings are identical to those of the GCR flux. In general, the LPF GCR flux depressions show a trend similar to those observed on polar and near-polar neutron monitors. Although the LPF spacecraft remained below the ecliptic for the period of the study reported here, no evident better agreement was found with South neutron monitor (i. e. Mc Murdo and Terre Adelie stations) observations with respect to those of northern stations (i. e. Thule and Oulu stations). Average depression characteristics are reported in Table 2. The interval of time during which the flux of GCRs remains depressed between decrease and recovery phases is called here *plateau*. The depression intensity was observed to be of 6%, on average. Earth neutron monitor observations, being representative of GeV GCR fluxes, present maximum depression intensities of 2%. In general, the dynamics of

Table 2. Characteristics of GCR short-term depressions observed with the PD aboard LPF.

	Duration (days)	%
Decrease	2.6±1.0	
Plateau	1.3±0.8	
Recovery	3.7±1.1	
Total	7.6±1.6	
Intensity		6.0±1.7

short-term variations with intensities smaller than 3% on LPF are not observed on Earth.

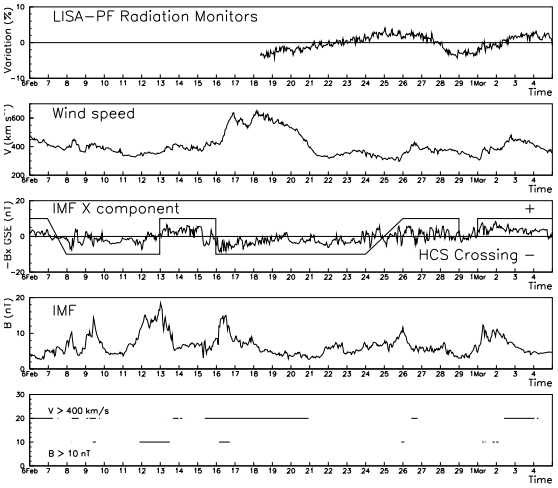

Figure 1. Comparison of LPF PD counting rate fractional variations with simultaneous ACE observations in L1 of solar magnetic field and wind plasma parameters during the Bartels rotation 2490 (February 6th, 2016 - March 4th, 2016).

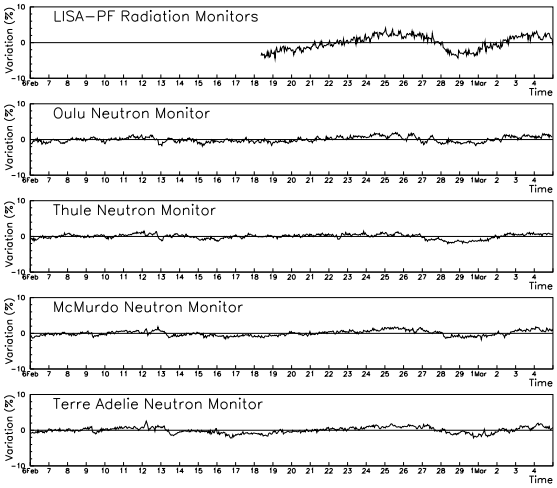

Figure 2. Comparison of LPF PD with neutron monitor data during the Bartels rotation 2490.

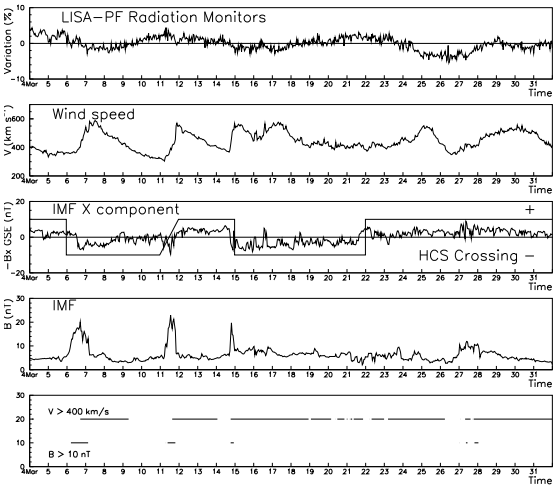

Figure 3. Same as Fig. 1, but during the Bartels rotation 2491 (March 4th, 2016 - March 31st, 2016).

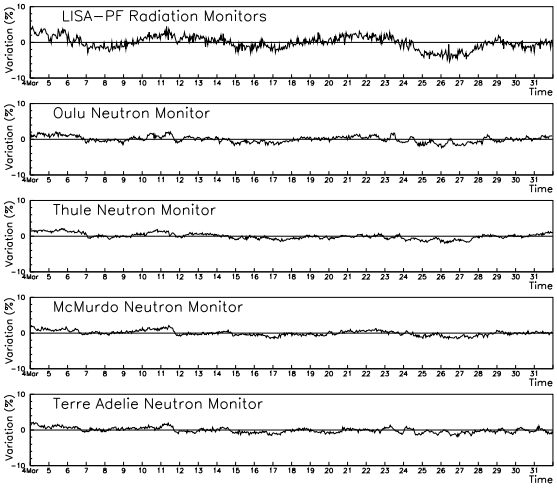

Figure 4. Same as Fig. 2, but during the Bartels rotation 2491.

4. Conclusions

The high counting rate PD placed aboard LPF allows for the measurement of GCR proton and helium flux oscillations compatible with the third harmonic of the Sun rotation period above 70

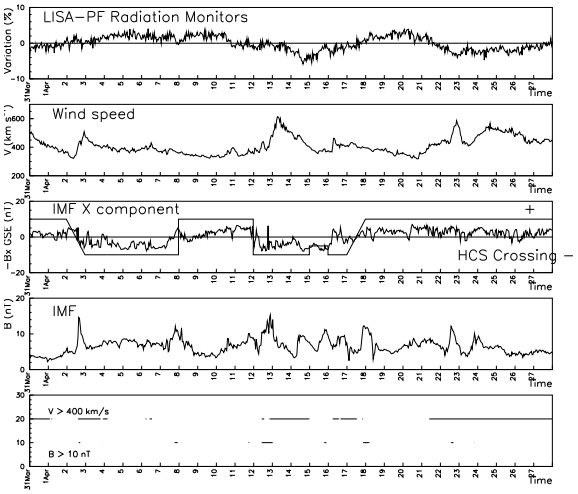

Figure 5. Same as Fig. 1, but during the Bartels rotation 2492 (March 31st, 2016 - April 27th, 2016).

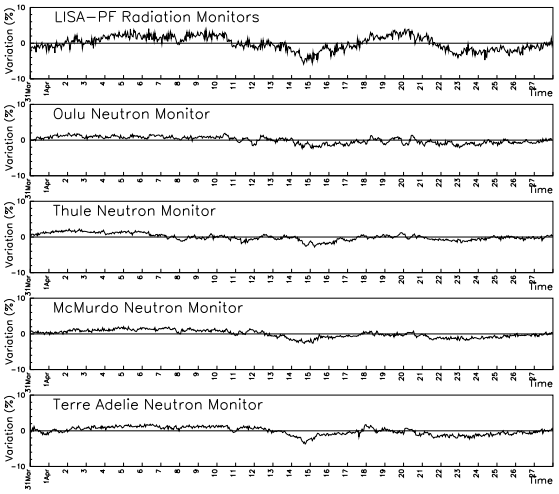

Figure 6. Same as Fig 2, but during the Bartels rotation 2492.

MeV n^{-1}. One-hour binned data present errors at percent level. GCR depressions under study appear to be correlated with an IMF intensity > 10 nT and/or a solar wind speed > 400 km s^{-1}. Their average intensity and duration are of (7.6±1.6) days and (6.0±1.7)%, respectively. Low-vertical geomagnetic cutoff neutron monitor observations show that these same depressions appear of just 2% above 5.5 GeV.

References

[1] Beer J 2000 *Cosmic Rays and Earth* J W Bieber, E Eroshenko, P Evenson, E O Flückiger and R Kallenbach eds. *Sp. Sc. Rev.* (Elsevier) **93**
[2] Shikaze Y *et al* 2007 *Astropart. Phys.* **28** 154-167
[3] Grimani C *et al* 2007 *Proc. 30th Int. Cosmic Ray Conf. (Merida)* **1** 485-488
[4] Grimani C 2004 *A&A* **418** 649-653
[5] Grimani C 2007 *A&A* **474** 339-343
[6] Nymmik R A *et al* 1999 *Proc. 26th Int. Cosmic Ray Conf. (Salt Lake City)* **6** 268-271
[7] Nymmik RA *et al* 1999 *Proc. 26th Int. Cosmic Ray Conf. (Salt Lake City)* **6** 280-283
[8] Gleeson L J and Axford W I 1968 *Ap. J.* **154** 1011-1026
[9] Sabbah I and Kudela K 2011 *J. Geophys. Res.* **116** A04103
[10] Richardson I G 2004 *Sp. Sc. Rev.* **111** 267-376
[11] Antonucci F *et al* 2011 *Class. Quantum Grav.* **28** 094001
[12] Antonucci F *et al* 2012 *Class. Quantum Grav.* **29** 124014
[13] M Armano *et al* 2016 *Phys. Rev. D* **116** 231101
[14] https://wolke7.aei.mpg.de/index.php/s/i6qxc8zNnOgGzKQ
[15] Shaul D *et al* 2006 *AIP Conf. Proc.* **873** 172-178
[16] Araújo H M *et al* 2005 *Astropart. Phys.* **22** 451-469
[17] Grimani C *et al* 2005 *Class. Quantum Grav.* **22** S327-S332
[18] Grimani C *et al* 2015 *Class. Quantum Grav.* **32** 035001
[19] Papini P, Grimani C and Stephens A S 1996 *Nuovo Cimento* **19** 367-387
[20] Cañizares P *et al* 2011 *Class. Quantum Grav.* **28** 094004
[21] Mateos I *et al* 2012 *J. Phys.: Conf. Ser.* **363** 012050
[22] Storini M *et al* 2008 *OPOCE publisher for COST 724 action* 63-69
[23] http://cosmicrays.oulu.fi/phi/Phi_mon.txt
[24] https://cdaweb.sci.gsfc.nasa.gov/index.html/